Current drag in a single quantum well

1996 J. Phys.: Condens. Matter 8 3705

(http://iopscience.iop.org/0953-8984/8/20/016)

J. Phys.: Condens. Matter **8** (1996) 3705–3714. Printed in the UK

Current drag in a single quantum well

E Söderström, A V Buyanov and Bo E Sernelius

Department of Physics and Measurement Technology, Linköping University, S-581 83 Linköping, Sweden

Received 22 January 1996

Abstract. We derive an expression for the contribution to the resistivity from the carrier–carrier scattering between two subbands with different masses in a single quantum well. The effects of the true wave functions of the carriers in the direction normal to the quantum well are taken into account. The calculations are done within the generalized Drude approach and with the RPA screening matrix. Numerical results for general temperatures are presented for a p-type centre-doped GaAs quantum well and compared with experiments.

1. Introduction

Recently the current drag between the carriers in two closely spaced quantum wells was demonstrated experimentally [1]. A current produced in one of the wells has the effect that the drifting carriers drag the carriers in the neighbouring well along. This drag occurs even if the carriers in the two wells have the same mass and charge. This type of drag effect had been predicted much earlier [2, 3], but the experimental verification inspired a fair amount of new both experimental [4] and theoretical work [5].

Related drag effects are well known in other experimental situations: phonons can be dragged along with drifting carriers: the minority carriers in a doped semiconductor can be dragged along with the drifting majority carriers with the striking result that the minority contribution to the conductivity is negative [6, 7]; drag effects modify the resistivities in heavily doped many-valley semiconductors [8].

In bulk material the carrier scattering has no direct contribution to the resistivity if all the carriers have the same mass-to-charge ratios. It has an indirect effect, though. It changes the distribution of the electrons and makes it closer to a thermal distribution in the centre-of-mass system [9]. This affects the carrier–impurity scattering and hence the resistivity. If the mass-to-charge ratio is different or, as in the pair of quantum wells, the carriers are separated in space, there is a direct contribution to the resistivity from the carrier–carrier scattering. In the present work we study a p-type doped GaAs quantum well with more than one quantized level occupied. The two lowest levels are formed from the two different hole bands. Thus, the masses of the two groups of carriers are different. Consequently this leads to a current drag effect for finite temperatures. Usually this carrier–carrier scattering is neglected in the theoretical treatment of the transport in a quantum well but we find that this contribution can be substantial.

In the first section we briefly discuss the system studied and outline how to find the energies and wave functions of the carriers in the different subbands. The rather subtle subject of the dynamical screening by all bands, taking the quasi-2D nature of the carriers into account, is discussed in more detail in the next section. We start then with the general

0953-8984/96/203705+10$19.50

case of N subbands contributing to the screening, and continue with a derivation of the explicit expressions for the special case of only two occupied subbands. The next section deals with the resistivity parallel to the doped plane. In order to calculate the contribution to the resistivity from the carrier–carrier scattering between two different subbands we first perform a very general derivation of the conductivity for a quasi-2D subband system for an unlimited number of bands, but without any scattering between the bands. This result has its own worth and serves as a starting point for further improvements, such as the subsequent examination of the effects of the carrier–carrier scattering, which is the main purpose of this study. Our results are presented and discussed and we compare the numerical calculations with experiment. Finally in the last section we summarize and draw conclusions.

2. The system studied and the carrier states

The resistivity derivations presented in this article are intended to be very general, but the numerical calculations are done for a 150 Å thick GaAs p-type quantum well where a 30 Å thick region in the middle of the well is doped. The well barriers are assumed to be high enough to be treated as infinite. The quantum well has the effect that the energy separation between the subbands is increased compared to a δ-doped layer in a bulk material. This means that fewer bands are populated. The effective masses of the heavy and light holes are $0.34m_e$ and $0.094m_e$, respectively, and the background screening $\mathcal{K}$ is set to 13.0. The system parameters are chosen in order to imitate the experimental set-up in [10], and at the end we compare our numerical results with the experimental data.

The carrier eigenstates are found by self-consistently solving the coupled Schrödinger and Poisson equations [11] in the direction normal to the quantum well. The exchange–correlation energy and the band non-parabolicity are ignored in the present calculations. The self-energy shifts due to exchange and correlation are not very important for the majority carrier bands [12] (the hole bands in the present case). The effects basically compensate by an inflow of carriers from outside the well leading to a Hartree contribution that to a large extent compensates the exchange–correlation potential. The minority carrier band on the other hand is affected more and there is a band-gap renormalization that affects optical experiments studying across-band-gap processes.

In figure 1 we present the self-consistent solutions for the centre-doped quantum well for three different doping concentrations at the temperature $T = 80$ K. Two heavy-hole and two light-hole subbands are included in the calculations. The energy scale is fixed by the potential which is set to zero at the edge of the well.

3. The screening

In a strict 2D model the unscreened carrier–carrier interaction, $v(\boldsymbol{q})$, between two carriers can regardless of participating subbands be considered as a simple Coulomb interaction between two point charges, i.e. $v(\boldsymbol{q}) = v_q/\mathcal{K}$, where $v_q = 2\pi e^2/q$ is the Fourier transform of the Coulomb interaction in 2D and $\mathcal{K}$ is the background screening. When the true wave functions of the carriers in the direction normal to the doped plane are taken into consideration one has to pay attention to which two subbands are actually involved in the process since each type of particle pair has different overlaps. The unscreened interaction between a carrier in subband i and another one in subband j has to be modified according

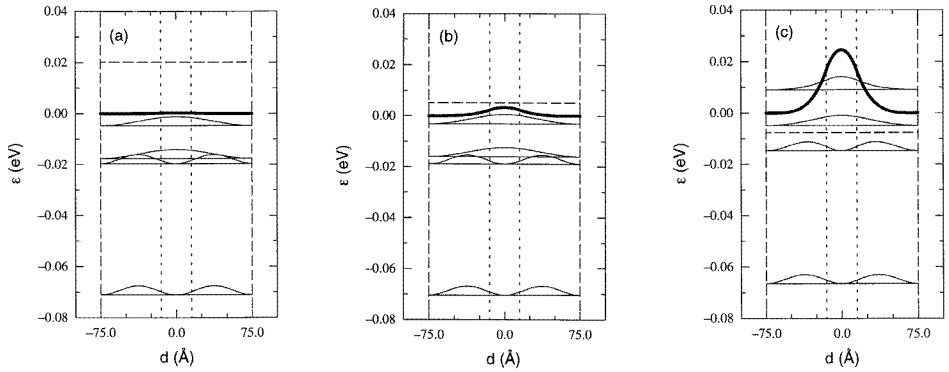

Figure 1. The self-consistent solutions at 80 K with four subbands for the doping concentrations 10^{17} cm^{-3} (a), 10^{19} cm^{-3} (b) and 10^{19} cm^{-3} (c). The dashed vertical lines indicate the quantum well, and the dotted vertical lines show the doped region in the middle of the well. The thick curve is the self-consistent Hartree potential. The thin curves represent the probability densities of the quantized levels. Each curve is shifted with the corresponding energy-level position. The carrier states are, from the top, heavy hole 1, light hole 1, heavy hole 2 and light hole 2. Note that the Fermi level, indicated with the dashed horizontal line, is below the light-hole-1 level for the highest carrier concentration, which explains the somewhat deviating results for that concentration.

to

$$\nu_{ij}(q) = \frac{\nu_q^{2D}}{\mathcal{K}} \int \int_{-\infty}^{\infty} \mathrm{d}z\, \mathrm{d}z' \varphi_i^{\dagger}(z)\varphi_i(z)\, \mathrm{e}^{-q|z-z'|} \varphi_j^{\dagger}(z')\varphi_j(z') \tag{1}$$

where $\varphi_i(z)$ is the wave function, discussed in the previous section, of the carriers in subband i in the direction normal to the quantum well. In our case the integrals are limited to the width of the quantum well. This bare carrier–carrier interaction is dynamically screened by all bands, which in the RPA implies that we sum over all so called bubble diagrams, or Coulomb self-energy insertions. In the strict 2D case with N subbands we have the screened interaction, indicated with a tilde, as

$$\tilde{\nu}(\boldsymbol{q},\, \omega) = \nu(q) \Big/ \left(1 - \sum_{j=1}^{N} g_j \nu(q) \chi_j^0(\boldsymbol{q},\, \omega)\right). \tag{2}$$

The quantity g_j is the degeneration of band j and the susceptibility χ_j^0 is given in the retarded form by

$$\chi_j^0(\boldsymbol{q},\, \omega) = \frac{2}{\hbar} \int \frac{\mathrm{d}^2 k}{(2\pi)^2} \left[\frac{n_F^j(\boldsymbol{k}) - n_F^j(\boldsymbol{k}+\boldsymbol{q})}{\omega - (\hbar/2m_j)[(\boldsymbol{k}+\boldsymbol{q})^2 - k^2] + \mathrm{i}\delta} \right] \tag{3}$$

where n_F is the Fermi occupation function. The dielectric function $\epsilon(\boldsymbol{q},\, \omega)$ can easily be found as the denominator of (2). We have neglected intersubband transitions and only included intrasubband transitions. We will stick to this approximation throughout. Interband transitions cannot be accommodated within the generalized Drude approach [13].

The quasi-2D case is more complicated since the interaction is dependent on which bands are participating. We get N sets of N coupled equations:

$$\tilde{\nu}_{ij}(q,\, \omega) = \nu_{ij}(q) + \sum_{k=1}^{N} g_k \nu_{ik}(q) \chi_k^0(q,\, \omega) \tilde{\nu}_{kj}(q,\, \omega) \tag{4}$$

for $i,\ j \in [1,\ N]$. Let us look at a specific j value. Then we have the N coupled equations

$$\begin{cases} \tilde{v}_{1j} = v_{1j} + \big(g_1 v_{11}\chi_1\big)\tilde{v}_{1j} + \ldots + \big(g_N v_{1N}\chi_N\big)\tilde{v}_{Nj} \\ \tilde{v}_{Nj} = v_{Nj} + \big(g_1 v_{N1}\chi_1\big)\tilde{v}_{1j} + \ldots + \big(g_N v_{NN}\chi_N\big)\tilde{v}_{Nj} \end{cases} \tag{5}$$

which in matrix formulation can be written as $A\tilde{\boldsymbol{\nu}}_j = \boldsymbol{\nu}_j$, where

$$A = \begin{bmatrix} (1+c_{11}) & c_{12} & \ldots & c_{1N} \\ & \vdots & & \\ c_{N1} & c_{N2} & \ldots & (1+c_{NN}) \end{bmatrix} \tag{6}$$

and $c_{ik} = -g_k v_{ik}\chi_k$. This is furthermore true for all j, which implies that we can reformulate the problem to a single matrix equation, $A\tilde{v} = v$, where v is a matrix containing all unscreened i–j interactions and $\tilde{v}$ is the corresponding screened results, which are what we are searching for. The solution is of course given by $\tilde{v} = A^{-1}v$. We have thus shown that it is possible to derive all dynamically screened carrier–carrier interactions, $\tilde{v}_{ij}(\boldsymbol{q},\ \omega)$, from all the unscreened results found from equation (1) by calculating and inverting the single matrix A, as defined in equation (6).

The scattering impurities are still assumed to be in a δ-layer. The unscreened interaction $u(q)$ between a carrier in subband i and the impurities has to be modified in the same manner as the carrier–carrier interaction if the true wave functions of the carriers in the direction normal to the doped plane are taken into account. The modified unscreened interaction becomes

$$u_i(q) = \frac{v_q^{2D}}{\mathcal{K}} \int_{-\infty}^{\infty} \mathrm{d}z \varphi_i^{\dagger}(z)\, \mathrm{e}^{-q|z|}\, \varphi_i(z) \tag{7}$$

where the integral again is limited to the quantum well in the current calculations. This time we only have *one* set of coupled equations, namely

$$\tilde{u}_i(\boldsymbol{q},\ \omega) = u_i(q) + \sum_{k=1}^{N} g_k v_{ik}(q)\chi_k^0(\boldsymbol{q},\ \omega)\tilde{u}_k(\boldsymbol{q},\ \omega) \tag{8}$$

where $i \in [1,\ N]$. An examination of (8) shows that we have the same relationship between the screened and the unscreened terms as in the carrier–carrier interaction, i.e. again we need to invert the matrix A given in (6) to get the dynamically screened carrier–impurity interaction $\tilde{u}(\boldsymbol{q},\ \omega)$.

Often the conductivity is dominated by the lowest subbands, especially in the low-temperature region. This is especially true when studying a quasi-2D system in a quantum well where the energy separation between the subbands becomes large. Therefore it is useful to derive the explicit expressions for the case of only two subbands. The carrier–carrier interaction and the carrier–impurity interaction are then found from the inverse of the (2×2) matrix

$$A = \begin{bmatrix} (1 - v_{11}\chi_1) & -v_{12}\chi_2 \\ -v_{21}\chi_1 & (1 - v_{22}\chi_2) \end{bmatrix} \tag{9}$$

which can easily be done analytically. The screened interaction within and between the two bands becomes

$$\begin{cases} \tilde{v}_{ii} = \big[\big(1 - v_{jj}\chi_j\big)v_{ii} + v_{ij}v_{ij}\chi_j\big] \big/ \big[\big(1 - v_{ii}\chi_i\big)\big(1 - v_{jj}\chi_j\big) - v_{ij}v_{ij}\chi_i\chi_j\big] \\ \tilde{v}_{ij} = v_{ij} \big/ \big[\big(1 - v_{ii}\chi_i\big)\big(1 - v_{jj}\chi_j\big) - v_{ij}v_{ij}\chi_i\chi_j\big] \end{cases} \tag{10}$$

where $i = 1,\ 2$ and $j \neq i$. The screened carrier–impurity interaction with the same restrictions on i and j is

$$\tilde{u}_i = \big[\big(1 - v_{jj}\chi_j\big)u_i + v_{ij}\chi_j u_j\big] \big/ \big[\big(1 - v_{ii}\chi_i\big)\big(1 - v_{jj}\chi_j\big) - v_{ij}v_{ij}\chi_i\chi_j\big]. \tag{11}$$

That the relative complexity of these terms is due to the quasi-2D nature of the carriers can be confirmed by replacing the modified bare interactions in the equations (10) and (11) with $v_q/\mathcal{K}$ which reduces the screened interactions to the strict 2D formula (2), as expected.

4. The resistivity calculations

First we derive an expression for the DC resistivity of a many-band quasi-2D system without any scattering between the subbands. The result is based on the generalized Drude approach (GDA) [13] and is valid for general temperatures and unlimited number of subbands. Secondly the effects of the scattering between two subbands are studied and an expression for the current drag effect is obtained. The true wave functions of carriers in the direction normal to the quantum well enters the resistivity calculation both through the modified bare interactions and through the RPA screening, which were both discussed in the previous section. Here we are not concerned about the explicit form of the interactions, just noting that $\tilde{v}_{ij}(\boldsymbol{q},\ \omega)$ stands for the screened interaction between a carrier in subband i and a carrier in subband j, and that $\tilde{u}_i(\boldsymbol{q})$ denotes the screened interaction between a carrier in subband i and an impurity.

For high frequencies it is possible to derive very rigorous results for the resistivity based on the Kubo formalism [14]. The basic idea in the GDA is to expand the simple Drude expression

$$\sigma_D(\omega) = \left(ne^2/m\right)/(1/\tau - \mathrm{i}\omega) \tag{12}$$

for high frequencies and compare it with the rigorous Kubo expression. An expression for the inverse relaxation time $1/\tau$, which is generalized to become frequency dependent, can be identified and put back into the original equation (12) for the dynamical conductivity. Finally it is assumed that the new expression $\sigma_{GDA}(\omega)$ is valid for *all* frequencies, especially the zero limit. The validity of this approach was studied earlier [15]. The GDA is related to memory function approaches to the conductivity [16].

To obtain the Kubo expression for the conductivity we follow the outline in [14], adjusting the derivation to the case of a many-band quasi-2D system [17]. We find

$$\sigma_{Kubo}(\omega) = \mathrm{i}\sum_i \frac{e^2 n_i g_i}{\omega m_i} + \mathrm{i}\frac{\Pi(\omega)}{\omega} \tag{13}$$

where the sum is over all N included subbands, n_i is the carrier concentration in subband i, and the current–current correlation function $\Pi(\omega)$ is given by

$$\begin{aligned}\Pi(\omega) = \sum_i g_i \frac{n_{imp}e^2}{4\pi m_i^2\omega^2}\int \mathrm{d}q\ S(q)q^3\tilde{u}_i^2(q)\Big[\chi_i^0(\boldsymbol{q},\ 0) - \chi_i^0(\boldsymbol{q},\ \omega)\Big] + \sum_{ij} g_i g_j \frac{n_{imp}e^2}{4\pi m_i m_j\omega^2} \\ \times \int \mathrm{d}q\ S(q)q^3\tilde{u}_i(q)\tilde{u}_j(q)\tilde{v}_{ij}(q,\ \omega)\Big[\chi_i^0(\boldsymbol{q},\ 0) - \chi_i^0(\boldsymbol{q},\ \omega)\Big] \\ \times\Big[\chi_j^0(\boldsymbol{q},\ 0) - \chi_j^0(\boldsymbol{q},\ \omega)\Big].\end{aligned} \tag{14}$$

Here $\tilde{u}_i(q)$ and $\tilde{v}_{ij}(q)$ are again the screened carrier–impurity and carrier–carrier interactions, respectively, g_j is the degeneracy, m_i is the effective mass of each subband, and n_{imp} is the total number of scattering centres, usually taken as the dopant concentration. The structure factor $S(q)$, which is a result of an assemble averaging of the impurity positions, is equal to one for randomly distributed impurities and will from now on be dropped.

The expression (13) should be compared with the high-frequency expansion of the Drude expression for many subbands, without any scattering between the groups of carriers,

$$\sigma_D^{high} = \sum_i \frac{n_i g_i e^2}{m_i \omega^2}\left[\frac{1}{\tau_i} + \mathrm{i}\omega\right] \tag{15}$$

and the inverse relaxation time for band i can be identified as

$$\begin{aligned}\frac{1}{\tau_i}(\omega) = \mathrm{i}\frac{n_{imp}}{4\pi n_i m_i \omega}\int \mathrm{d}q\, q^3 \tilde{u}_i^2(q)\Big(\chi_i^0(\boldsymbol{q},\,\omega) - \chi_i^0(\boldsymbol{q},\,0)\Big) + \mathrm{i}\sum_j g_j \frac{n_{imp}}{4\pi n_i m_j \omega} \\ \times \int \mathrm{d}q\, q^3 \tilde{u}_i(q)\tilde{u}_j(q)\tilde{\nu}_{ij}(q,\,\omega)\Big[\chi_i^0(\boldsymbol{q},\,0) - \chi_i^0(\boldsymbol{q},\,\omega)\Big] \\ \times\Big[\chi_j^0(\boldsymbol{q},\,0) - \chi_j^0(\boldsymbol{q},\,\omega)\Big].\end{aligned} \tag{16}$$

The above expression should be inserted back into the original Drude expression (15) and after taking the DC limit we are left with

$$\sigma_{GDA}(0) = \sum_j g_j\Big(4\pi n_j^2 e^2/n_{imp}\Big)\Big/\left(\int \mathrm{d}q\, q^3\left\{-\frac{\partial}{\partial\omega}\,\Im\,\chi_j^0(q,\,\omega)\right\}_{\omega=0}\tilde{u}_j^2(q)\right) \tag{17}$$

since the second term in (16) vanishes in the zero-frequency limit. Finally, the total resistivity $\varrho(0)$ is found from the inverse of the conductivity (17) and the first part of our derivation is done.

To obtain the effect of the current drag from the scattering between the bands, with the present limitation of including only two subbands in the calculations, we generalize the results of [8] for arbitrary concentrations to obtain the dynamical Drude conductivity with scattering between two bands as

$$\sigma_D(\omega) = \frac{\frac{n_1e^2}{m_1}\left[\frac{1}{\tau_2} - \mathrm{i}\omega\right] + \frac{n_2e^2}{m_2}\left[\frac{1}{\tau_1} - \mathrm{i}\omega\right] + \frac{(n_1+n_2)^2e^2}{[n_1m_1+n_2m_2]}\frac{1}{\tau_{12}}}{\left[\frac{1}{\tau_1} - \mathrm{i}\omega\right]\left[\frac{1}{\tau_2} - \mathrm{i}\omega\right] + \frac{m_1m_2}{[n_1m_1+n_2m_2]}\frac{1}{\tau_{12}}\left\{\frac{n_2}{m_1}\frac{1}{\tau_2} + \frac{n_1}{m_2}\frac{1}{\tau_1}\right\} - \mathrm{i}\omega\frac{1}{\tau_{12}}} \tag{18}$$

where τ_{12} is the scattering time between the two groups of carriers. The high-frequency expansion of the Drude conductivity becomes

$$\sigma_D^{high} \approx \frac{n_1e^2}{m_1\omega^2}\left\{\frac{1}{\tau_1} + \mathrm{i}\omega\right\} + \frac{n_2e^2}{m_2\omega^2}\left\{\frac{1}{\tau_2} + \mathrm{i}\omega\right\} + \frac{n_1m_1n_2m_2}{(n_1m_1+n_2m_2)}\left(\frac{1}{m_1} - \frac{1}{m_2}\right)^2\frac{e^2}{\omega^2}\frac{1}{\tau_{12}} \tag{19}$$

where the first two terms are the contributions from the impurity scattering and the third term is the contribution from the carrier–carrier scattering.

The impurity-scattering terms should again be compared with the Kubo expressions for impurity scattering and the inverse relaxation times are given by (16), but the third term from the carrier–carrier scattering must be compared with the Kubo expression for a multi-component plasma. With suitable modifications in the derivation of the first integral of (2.30) in [14], taking the quasi-2D nature of the system into account [17], one gets with our notations in the zero-frequency limit

$$\begin{aligned}\frac{n_1m_1n_2m_2}{(n_1m_1+n_2m_2)}\left(\frac{1}{m_1} - \frac{1}{m_1}\right)^2\frac{e^2}{\omega^2}\frac{1}{\tau_{12}} = \frac{4e^2\hbar}{\omega^3}\left[\frac{1}{m_1} - \frac{1}{m_2}\right]^2\int\frac{\mathrm{d}^2q}{(2\pi)^2}q_\mu^2\int_0^\infty \\ \times\frac{\mathrm{d}\omega'}{(2\pi)}\frac{\beta\hbar\omega/2}{\sinh^2(\beta\hbar\omega'/2)}\big|\tilde{\nu}_{12}(\omega')\,\Im\big[\chi_1(\omega')\big]\,\Im\big[\chi_2(\omega')\big]\end{aligned} \tag{20}$$

where $\beta = 1/k_B T$ and q_μ is the projection of the wave vector on the applied electric field $\boldsymbol{E}$. The DC relaxation time for the carrier–carrier scattering is identified as

$$\frac{1}{\tau_{12}}(0) = 2\beta\hbar^2 \frac{(n_1 m_1 + n_2 m_2)}{n_1 m_1 n_2 m_2} \int \frac{\mathrm{d}^2 q}{(2\pi)^2} q_\mu^2 \times \int_0^\infty \frac{\mathrm{d}\omega}{(2\pi)} \frac{|\tilde{v}_{12}(\boldsymbol{q}, \omega)|^2 \, \Im[\chi_1(\boldsymbol{q}, \omega)] \, \Im[\chi_2(\boldsymbol{q}, \omega)]}{\sinh^2(\beta\hbar\omega/2)}. \tag{21}$$

The final step is to insert the above-derived relaxation time into the low-frequency limit of the Drude expression (18). Thus the inverse relaxation time (21) should be inserted into

$$\sigma_{GDA}(0) = \frac{n_1 e^2}{m_1}\tau_1 + \frac{n_2 e^2}{m_2}\tau_2 - n_1 n_2 e^2 \left[\frac{1}{m_1}\tau_1 - \frac{1}{m_2}\tau_2\right]^2 \Bigg/ \left(\left\{ \frac{n_2}{m_1}\tau_1 + \frac{n_1}{m_2}\tau_2 \right\} + \tau_{12} \left\{ \frac{n_2}{m_1} + \frac{n_1}{m_2} \right\} \right) \tag{22}$$

which with obvious notation can be rewritten as

$$\sigma_{GDA}(0) = \sigma_1 + \sigma_2 - \frac{\left[n_2\sigma_1 - n_1\sigma_2\right]^2}{\left(\left\{ n_2^2\sigma_1 + n_1^2\sigma_2 \right\} + n_1 n_2 e^2 \tau_{12} \left\{ \left(n_1 m_1 + n_2 m_2\right)/m_1 m_2 \right\} \right)} \tag{23}$$

where σ_i, $i = 1, 2$, are explicitly given by (17). The two limits of vanishing and strong carrier–carrier interactions are

$$\begin{cases} \sigma_{GDA}(0) \to \sigma_1 + \sigma_2 & \tau_{12} \to \infty \\ \sigma_{GDA}(0) \to \left(n_1 + n_2\right)^2 \Big/ \left(n_1^2/\sigma_1 + n_2^2/\sigma_2 \right) & \tau_{12} \to 0. \end{cases} \tag{24}$$

Finally, the last term in the denominator of (23) is after the angular integration given by:

$$n_1 n_2 e^2 \tau_{12} \left\{ \frac{n_1 m_1 + n_2 m_2}{m_1 m_2} \right\} = \left(n_1 n_2 2\pi e^2/\beta\hbar^2\right) \Bigg/ \left(\int \mathrm{d}q q^3 \int_0^\infty \times \frac{\mathrm{d}\omega}{(2\pi)} \frac{|\tilde{v}_{12}(\boldsymbol{q}, \omega)|^2 \, \Im[\chi_1(\boldsymbol{q}, \omega)] \, \Im[\chi_1(\boldsymbol{q}, \omega)]}{\sinh^2(\beta\hbar\omega/2)} \right). \tag{25}$$

5. Results

We have performed several calculations for the ideal system described in section 2, similar to the experimental one [10], in order to study our theoretical results. We have used the 3D acceptor concentrations 10^{17}, 10^{18} and 10^{19} cm^{-3}, assuming that each acceptor contributes with exactly one carrier, and varied the temperature between 4 and 300 K. The corresponding 2D concentrations are found from the 3D ones through multiplication by the width of the doped region. In a real experiment only a small fraction of the acceptors are ionized at low temperatures. We have also performed calculations for the more realistic system with additional scattering centres, simulating unintentional doping, and included the scattering against non-ionized impurities, and compared our numerical results with the experimental data.

In figure 2 we compare the quasi-2D resistivity with the strict 2D results for three different concentrations. We also distinguish between the case when only the two lowest subbands are included in the calculations, and the case when also the next pair of subbands contributes to the resistivity. For the highly doped system the conductivity contribution from the second pair of occupied hole states dominates in the high-temperature region, which explains the anomalous behaviour of these curves.

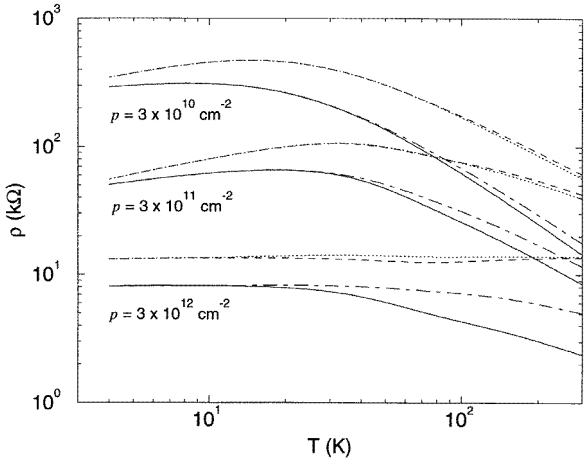

Figure 2. The total resistivity without any scattering between the bands. The solid curves are the full results with four subbands included in the calculations while the dotted–dashed curves are the corresponding results with only two subbands. The dashed and the dotted curves are the strict 2D results for four and two bands, respectively.

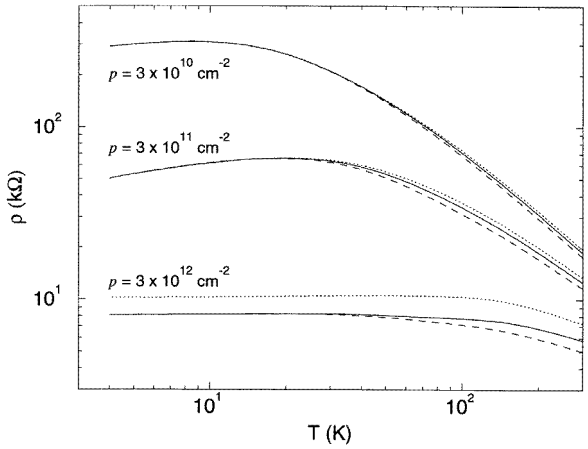

Figure 3. The effects of the current drag on the total resistivity. The solid curves are our full results with scattering between the bands. The dashed curves are our earlier results for the quasi-2D system with two subbands but without any scattering between the subbands, and the dotted curves are the corresponding results in the limit of very strong scattering between the bands; this demonstrates the result with maximum possible drag effect.

The calculations with the full carrier–carrier interaction included are presented in figure 3, where also the two limits from equation (24) with vanishing and very strong interaction are shown. From equation (22) we note that the carrier–carrier contribution always increases the resistivity, but the maximum effect of the current drag is always limited by (24).

Finally, in figure 4 we compare our numerical results with experimental data [10], where the given doping levels are 3×10^{11} cm^{-2} (1×10^{18} cm^{-3}) in (a) and 9×10^{9} cm^{-2}

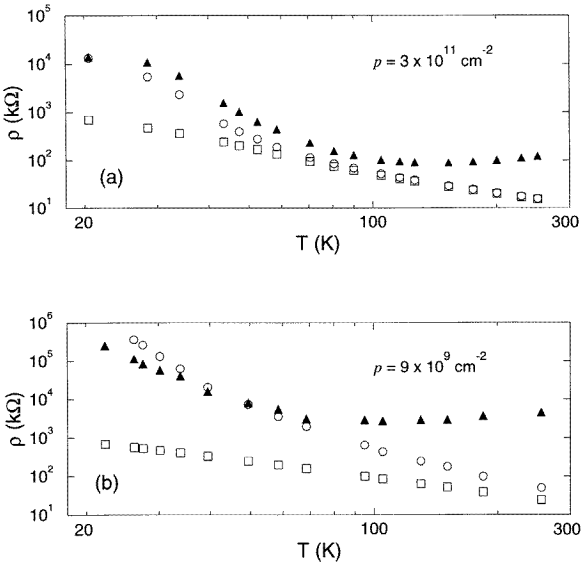

Figure 4. A comparison with experiment. The open squares are our results with two subbands included in the calculations. The filled triangles are the experimental data. The open circles are the calculated resistivities in the presence of $\mathcal{N} = 5 \times 10^{15}$ cm^{-3} additional scattering centres, simulating unintentional doping.

(3×10^{16} cm^{-3}) in (b). The experimental values of the resistivity are illustrated with filled triangles while our calculations for two subbands with carrier–carrier scattering are presented as open squares. We have at each point used the measured carrier concentration since it varies considerably with the temperature. In order to imitate a true sample and to illustrate the effects of unintentional doping we have also calculated the resistivity with 5×10^{15} cm^{-3} additional ionized impurities in the quantum well, not contributing to the carrier concentration but interacting with the carriers and thus increasing the resistivity. The last results are given by the open circles and they are in satisfactory agreement with the experiments. The interaction with the non-ionized impurities can be neglected [17].

The calculations were performed ignoring the phonons, which explains the deviations from the experimental values in the high-temperature limit. Unfortunately, this is also the region where the current drag is most noticeable. One should extend the theory to include the phonons to be able to confirm the effect of the current drag in the studied system. There are also several other unknown factors which could account for the divergence with the experiments, such as the uncertainty in the true width of the doped layer and scattering against edge defects of the quantum well. We have also omitted multiple scattering, which ought to affect the transport properties in the low-doping limit.

6. Summary and conclusions

We have derived a general expression for the resistivity of a many-subband quasi-2D system which takes the true wave functions of the carriers in the direction normal to the doped plane into account. The derivation is based on the generalized Drude approach with the temperature dependent RPA screening matrix. Transport properties of multisubband systems

have been studied earlier at zero temperature [18] but to our knowledge this is the first time an expression valid for all temperatures and an unlimited number of subbands is obtained.

We have also derived the effects of the carrier–carrier scattering, or current drag, between two subbands with different masses, also within the generalized Drude approach with the temperature dependent RPA screening matrix and with the true wave functions of the carriers in the direction normal to the doped plane. We have found that the resistivity is increased by a temperature dependent factor which we have calculated for a p-type centre-doped GaAs quantum well. The current drag effect is found to be negligible for low temperatures but substantial for temperatures close to room temperature.

Acknowledgment

Financial support from the Swedish National Science Research Council is gratefully acknowledged.

References

[1] Gramila T J, Eisenstein J P, MacDonald A H, Pfeiffer L N and West K W 1991 *Phys. Rev. Lett.* **66** 1216
[2] Progrebinskii M B 1977 *Fiz. Tekh. Poluprovodn.* **11** 637 (Engl. transl. *Sov. Phys.–Semicond.* **11** 372)
[3] Price P J 1983 *Physica* B **117** 750
[4] Sivan U, Solomon P M and Shtrikman H 1992 *Phys. Rev. Lett.* **68** 1196
[5] Laikhtman B and Solomon P M 1990 *Phys. Rev.* B **41** 9921
Boiko I I and Sirenko Yu M 1990 *Phys. Status Solidi* **159** 805
Solomon P M and Laikhtman B 1991 *Superlatt. Microstruct.* **10** 89
Rojo A G and Mahan G D 1992 *Phys. Rev. Lett.* **68** 2074
Maslov D I 1992 *Phys. Rev.* B **45** 1911
Duan J M and Yip S 1993 *Phys. Rev. Lett.* **70** 3647
Cui H L, Lei X L and Horing N J M 1993 *Superlatt. Microstruct.* **13** 221
Shimshoni E and Sondhi S L 1994 *Phys. Rev.* B **49** 11 484
Flensberg K and Hu B Yu-K 1994 *Phys. Rev. Lett.* **73** 3572
[6] Höpfel R A, Shah J, Wolf P A and Gossard A C 1986 *Phys. Rev. Lett.* **56** 2736; 1988 *Phys. Rev.* B **37** 6941
[7] McLean T P and Paige E G S 1960 *J. Phys. Chem. Solids* **16** 220
[8] Sernelius B E 1990 *Phys. Rev.* B **41** 3060
[9] Sernelius B E and Söderström E 1991 *J. Phys. C: Solid State Phys.* **3** 842
[10] Buyanov A, Ferreira A C, Söderström E, Buyanova I A, Holtz P O, Sernelius B E, Monemar B, Sunderam M, Campman K, Mertz J L and Gossard A C 1996 *Phys. Rev.* B **53** 1357
[11] Ando T, Fowler A B and Stern F 1982 *Rev. Mod. Phys.* **54** 437
[12] Linnerud I 1994 *PhD Thesis* University of Trondheim
[13] Sernelius B E 1989 *Phys. Rev.* B **40** 1243
[14] Sernelius B E 1987 *Phys. Rev.* B **36** 1080
[15] Sernelius B E and Söderström E 1991 *J. Phys. C: Solid State Phys.* **3** 1493
[16] Götze W and Wölfe P 1972 *Phys. Rev.* B **6** 1226
[17] Söderström E 1996 unpublished notes
[18] Hai G Q, Studart N and Peeters F M 1995 *Phys. Rev.* B **52** 8363